

Rectifying memristor bridge circuit realized with human skin

Oliver Pabst^{1,2}

1. Department of Physics, University of Oslo, Oslo, Norway
2. E-mail any correspondence to: oliverpa@mail.uio.no

Abstract

It has been demonstrated before that human skin can be modeled as a memristor (memory resistor). Here we realize a memristor bridge by applying two voltages of opposite signs at two different skin sites. By this setup it is possible to use human skin as a frequency doubler and half-wave rectifier which is an application of the non-linear electrical properties of human skin. The corresponding electrical measurements are non-linear since these are affected by the applied stimulus itself.

Keywords: Bioimpedance; non-linear electrical measurements; human skin; memristor; rectification

Introduction

A memristor (**memory resistor**) is labelled as the fourth passive electrical circuit element [1] and its resistance may change with an applied electrical voltage or current. It is characterized by its state dependent Ohm's law and its state equation that describes how the inner state changes with the applied electrical stimulus

$$v = M(\mathbf{x})i \quad (1)$$

$$\frac{d\mathbf{x}}{dt} = f(\mathbf{x}, i). \quad (2)$$

Equations (1) and (2) describe a generic memristor which is the second most general memristor type [2] and its memristance, $M(\mathbf{x})$, (in analogy to resistance) depends on \mathbf{x} , a vector of state variables. In analogy to the conductance of a resistor, a memristor can also be described by its memductance, $G(\mathbf{x})$, (state dependent conductance). However, any memristor exhibits a pinched hysteresis loop in the voltage current plot (V-I plot) with pinched point

position in the origin of coordinates ("fingerprint" of a memristor [3]). The branches of the loop can either cross the pinched point with different slopes (transversal memristor) or touch it with equal slopes (tangential memristor). A first realization of a memristor was presented in 2008 [4], which was based on titanium dioxide. Memristors based on other materials like tantalum oxide [5, 6], zinc oxide [7] or biological memristors such as the Venus flytrap [8] and slime mold memristors [9] have been demonstrated, as well. Other research is focused on implementation of memristors in electrical circuits that are used for neuromorphic computing [10-12] or emulating arithmetic operations [13, 14], as some examples.

This paper focuses on a 4-memristor bridge circuit (similar to a Wheatstone bridge but based on transversal memristor models instead of resistors, see Fig. 1a) that was used for synaptic weight programming in [15]. The same circuit was used for the generation of nth-order harmonics and frequency doubling in [16] and as full-wave rectifier in [17]. Here this circuit (in a two memristor configuration, see [17] and Fig. 1b) is realized with human skin (see Fig. 1c). Human skin exhibits non-linear electrical properties if the applied stimulus is large enough [18-20]. It was concluded that the sweat ducts in human skin can be modelled as a memristor [21]. As it was shown later, human skin actually contains two different memristor types, one based on electro-osmosis within the sweat ducts and one based on thermal changes within the stratum corneum [22]. Both are electrically in parallel to each other and the sweat duct memristor usually dominates the measurement as long as the galvanic contact through the sweat ducts is given. The memductance of the sweat duct memristor increases or

decreases, dependent on the sign of the applied voltage (or current) and the corresponding pinched hysteresis loop in the V-I plot is transversal [22]. The stratum corneum memristor experiences a memductance increase independent of the sign of the applied voltage and its pinched hysteresis loop is tangential [22]. The functioning of the here implemented memristor bridge depends on the physical conditions of the skin. If the galvanic contact through the sweat ducts is given under both corresponding electrodes (CC1 and CC2, see Fig. 1c), similar functioning as in [15-17] may be archived by the implemented circuit.

Measurements were done on 28 test subjects with constant amplitude (+1 V and -1 V) sinusoidal voltages of different very low frequencies that were applied via surface electrodes (see Fig. 1c). The currents recorded from some subjects were (more or less) half-wave rectified and for some other subjects the obtained currents had double the frequency as the applied voltages. A parameter that reflects the amount of rectification is introduced and used for quantitative analysis. The recordings here are affected by the applied voltage itself and can consequently be seen as non-linear electrical measurements (on human skin) [22]. Furthermore, these can be seen as part of Bioimpedance, since this field encompasses the passive electrical properties (memristor = fourth passive electrical circuit element) of organic tissues and corresponding recording techniques [23].

Materials and methods

Subject recruitment, approval

The measurements were conducted on 28 test subjects (16 male, 12 female, mean age 31 years, SD=9.5 years; all gave informed consent for participation in the study) at the University of Oslo in November and December in 2016. The study was performed in accordance with the guidelines given by the South-Eastern Review Board (REC South East) of the Regional Committees for Medical and Health Research Ethics in Norway. An approval of the study protocol by the committee was not required since this study is not falling under the definition of clinical research, but the research group was responsible for ensuring electrical safety for the test subjects.

Experimental Design

The measurements were either performed at the preferred or non-preferred hand side (randomly chosen). The results here were obtained from the third experiment of a test session that had an overall duration of one hour (the results from the first experiment are presented in [22] and within the second experiment, direct current (DC) voltage pulses with pulse heights of +0.8 V and -0.8 V were applied to the skin, unpublished results). After the experiment with the DC pulses (before this experiment started), all electrodes were disconnected from the instrumentation (but remained at the skin of the test subjects), and the test subjects were asked

to perform a one-minute workout on a stationary bike. After the test subjects completed the workout, the electrodes were connected to the instrumentation as illustrated in (Fig. 1c).

Within this experiment, two sinusoidal voltages (v_{CC1} and v_{CC2} , see Fig. 1) of the same frequency, and same amplitude as 1 V but opposite signs (phase shift of 180 degree, it was randomly chosen whether v_{CC1} or v_{CC2} started with the negative half of the period; the other voltage started with the positive half of the period, respectively) were applied for two periods. This procedure was performed three times for different frequencies (0.005 Hz, 0.05 Hz and 0.5 Hz) in randomized order. The time between runs during which no voltage was applied was 4 seconds.

Instrumentation

A custom-built measurement system (see Fig. 1c top) was used for the recordings. A data acquisition card (DAQ) (type USB-6356 from National instruments) enabled the application of two constant voltages and simultaneous reading (both was performed with 500 samples per period). The DAQ was connected to a personal computer and controlled by a custom-made software, which was written in NI LabVIEW (version 2014). The generated voltages v_{CC1} and v_{CC2} were provided at the "out1" and "out2" ports, respectively. The provided voltage v_{CC1} was read at the channel "In1" to measure the delay from signal generation inside the DAQ to actual provision by the analog-to-digital converter. A transimpedance amplifier (with $R_{fb} = 56 \text{ k}\Omega$) was used to convert the current, i , through the skin into a voltage that can be read by the DAQ (input "In2"). With the small capacitance $C_{fb} = 4.7 \text{ nF}$ in parallel, high frequency noise was reduced in addition. To ensure separation between the mains and the test subjects, the personal computer, monitor and data acquisition box were powered by an international medical isolation device (IMEDe 1000 from Noratel AG, Germany). Furthermore, current paths through the heart were avoided by placing all electrodes at the same side of the body.

The two voltages v_{CC1} and v_{CC2} were applied to the skin via the electrodes CC1 and CC2 (see Fig. 1c). Both were prewired, dry Ag/AgCl electrodes (from Wuhan Greentek PTY LTD), had an active area of 0.283 cm^2 , and were taped to the skin of the test subjects. After the experiment, the electrodes were cleaned for reuse (by wiping the electrodes with a cotton-wool ball that was soaked with ethanol). The electrode CC2 was placed at the forehead above the iris of the eye, at approximately the width of two fingers above the eyebrow. The electrode CC1 was either placed at the earlobe (variant A in Fig. 1c, for the first 12 out of 28 subjects) or at the forehead, approximately 0.5 centimeters downward with respect to CC2 and about 2 cm toward the outer part of the head (variant B in Fig. 1c, for the last 16 out of 28 subjects).

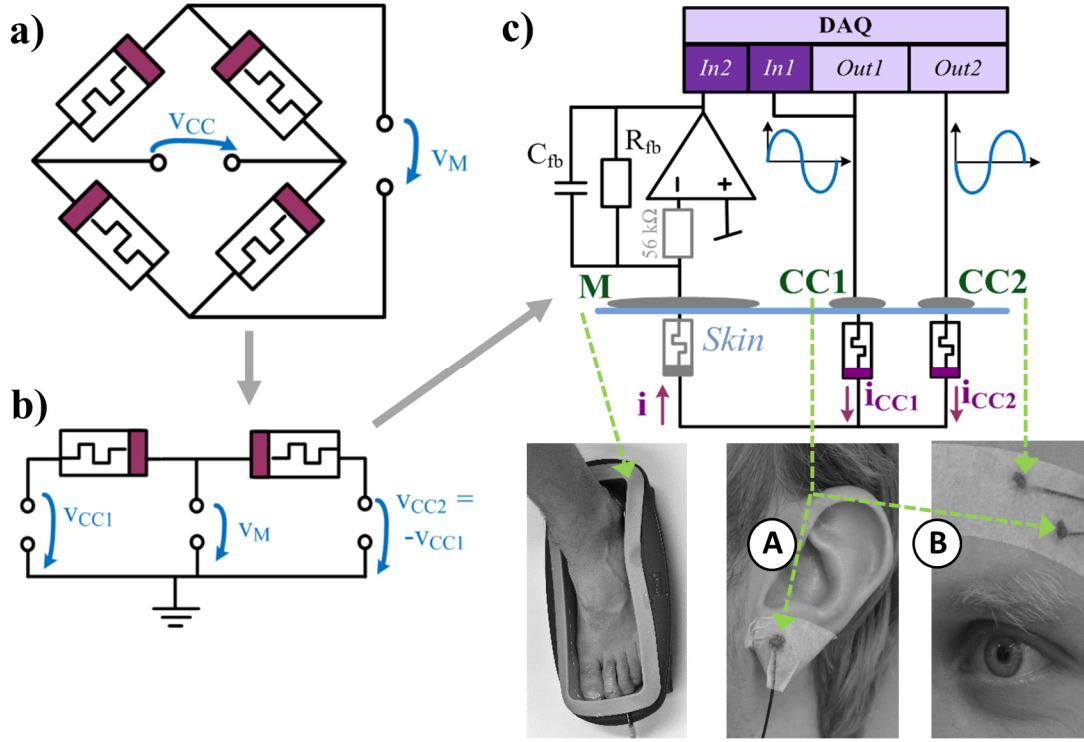


Fig. 1 | Memristor bridge circuit and its implementation on human skin (a) Schematic of the four memristor bridge circuit similar to the ones presented in [15-17] with voltage source V_{CC} and measured voltage V_M . (b) The two memristor version of the memristor bridge is realized by using two voltage sources with opposite sign as illustrated in the schematic (see also [17]). (c) Memristor bridge circuit realized with human skin. Schematic of the instrumentation (top) and the corresponding electrode placement (bottom) is shown for the left-hand side. The electrode setup on the right-hand side was equivalent. Voltages V_{CC1} and V_{CC2} were applied at the CC1 and CC2 electrodes, respectively. The CC1 electrode was attached to the earlobe (variant A, chosen for 12 out of 28 subjects) or to the forehead (variant B, chosen for 16 out of 28 subjects). The CC2 electrode was always placed at the forehead. All electrodes were put in place right after each other. The stratum corneum memristor and the sweat duct memristor (under each electrode) are electrically in parallel to each other and can be modeled as one overall memristor due to the closure theorem [1]. The greyed memristor symbol under the M electrode shall illustrate that the influence of the corresponding skin to the measurement is negligible. The direction of the voltage here is from skin surface (under CC1 and CC2) to deeper skin layers while it was from deeper skin layers to skin surface in the setup used in [22]. The same photograph that illustrates the electrode placement at the earlobe has been presented in [22] under Creative Commons Attribution 4.0 International License.

A tub filled with saline solution (0.9% NaCl, electrical contact was realized by 6 Ag/AgCl electrodes that were placed at the well of the tub) in which the foot was placed was used as a large M-electrode to minimize the contribution of the corresponding skin memristor to the measurement (see [24]).

Resulting current and parameterization

The measured current, i , (see Fig. 1c) is the sum of the currents through the skin under both, the CC1 and CC2, electrodes and can be expressed by

$$i = i_{CC1} + i_{CC2} \quad (3)$$

$$i = V_{CC1} \cdot G_{CC1}(x_1) + V_{CC2} \cdot G_{CC2}(x_2) \quad (4)$$

with $G_{CC1}(x_1)$ and $G_{CC2}(x_2)$ as the memductances under CC1 and CC2 respectively. Equation (4) can be simplified to

$$i = V_{CC1} (G_{CC1}(x_1) - G_{CC2}(x_2)) \quad (5)$$

since the voltage V_{CC2} is equal to $-V_{CC1}$. Thus, the current, i , will become 0 μA as the voltage V_{CC1} becomes 0 V and also

when the memductances under both electrodes (CC1 and CC2) obtain equal values. The measure, r_i , with

$$r_i = \left| \frac{1}{\hat{I} \cdot T} \int_0^T i \cdot dt \right| \quad (6)$$

shall be introduced for the quantitative analysis. This is the ratio of the area under the obtained current (in the current-time plot, see examples in Fig. 2) of one period normed by the duration of the period, T , ($T=1/f$) and the largest absolute value, \hat{I} , that the current obtains during this period. The area under each current was computed by the *trapz* function in Matlab (version 2016b).

The average rectified value of a sinusoidal signal normed by its amplitude is 0.6366 (see equation (9) in the supplementary information) and may be used for scaling:

$$r_{rec} / \% = \frac{r_i}{0.6366} \cdot 100 \quad (7)$$

The ratio of rectification, r_{rec} , obtains a value of 100% if the measured current is sinusoidal but (perfectly) full-wave rectified. If the current is sinusoidal but not rectified (and has no DC offset), r_{rec} will obtain a value of 0%.

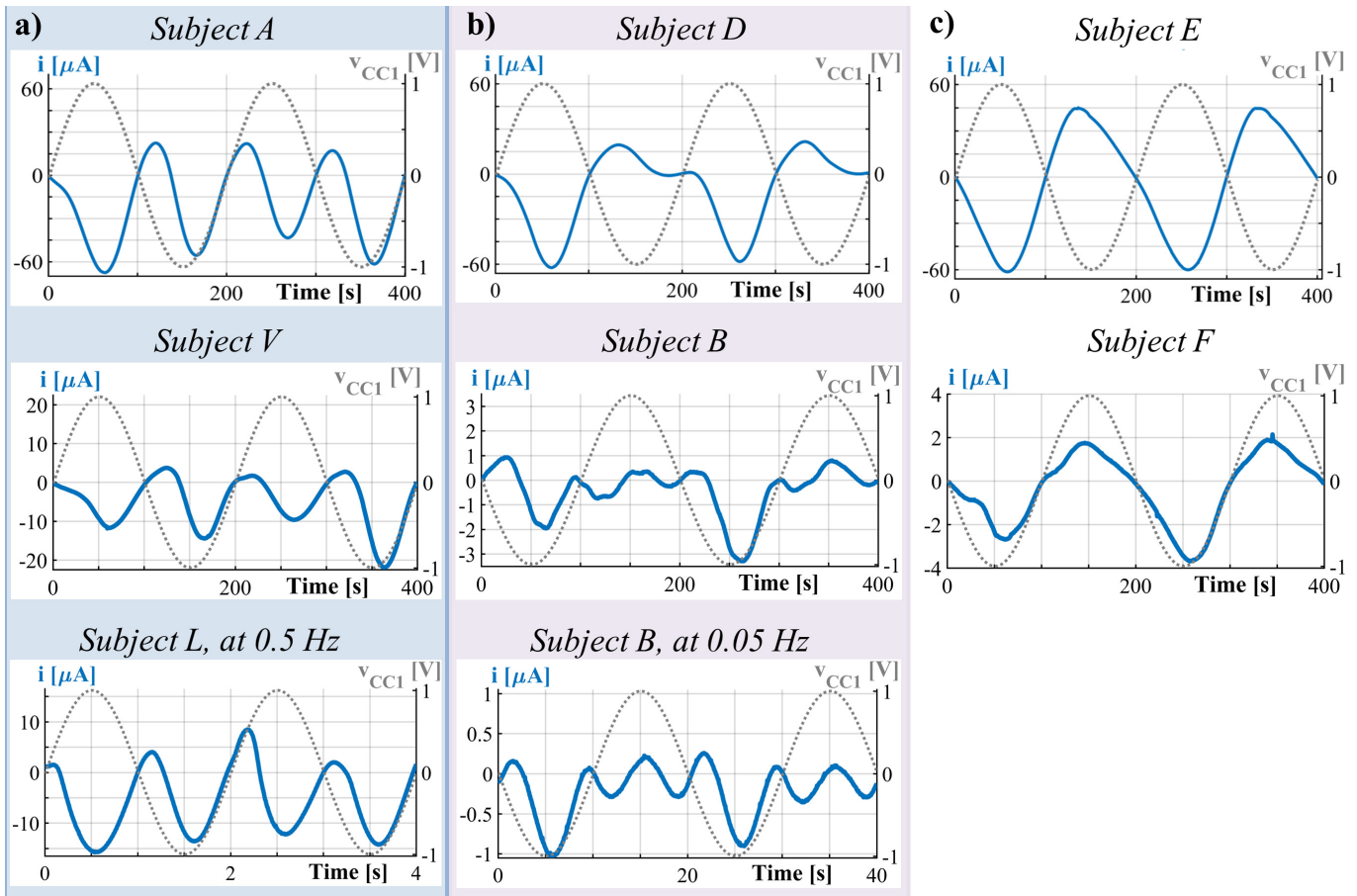


Fig. 2 | Results from several subjects. Applied sinusoidal voltage, v_{CC1} , (on CC1) and measured current, i , over time. The sign of the amplitude of v_{CC1} was either 1 V (subject A, for example) or -1 V (subject B, for example) due to randomization and the sign of v_{CC2} was always opposite. In the top and middle line, the results of the recordings with a voltage frequency of 0.005 Hz are shown. Subject labelling is in accordance with the results presented in [22]. The applied voltages themselves affect the memductance of the skin and consequently the resulting current (non-linear electrical measurement). The memductance changes during the recording and can be different at the beginning of the second period which explains also the differences in the recorded current from period to period. (a) Subject A, and V at 0.005 Hz and Subject L at 0.5 Hz. The frequency of the measure is double the frequency of the applied voltages. The measured currents of a total of five subjects (2 out of 12 with the CC1 electrode at the earlobe, 3 out of 16 with the CC1 electrode at the forehead) are comparable when the applied voltage frequency is 0.005 Hz. Two of these subjects show similar results at 0.05 Hz, and one of these two even shows a similar result at 0.5 Hz (subject L). (b) Subject D and B at 0.005 Hz and subject B at 0.05 Hz. The measured current has a large magnitude in one half of the period and is more or less cut off during the other half of the period. Six subjects in total (3 out of 12 with the CC1 electrode at earlobe, 3 out of 16 with the CC1 electrode at the forehead) show a similar behavior at a frequency of 0.005 Hz and five out of them show also (more or less) similar behavior at 0.05 Hz. (c) Subject E and F. The measured currents are non-linear, but neither half-wave rectification nor frequency doubling is observed. Seventeen subjects in total show similar behavior at 0.005 Hz.

Results

The results depend on the initial conditions of the skin and may be categorized into three groups.

Frequency doubling or (almost) full wave rectification

The results in Fig. 2(a) demonstrate that the implemented human skin memristor circuit can function more or less as a frequency doubler or full wave rectifier. The prerequisite for this functioning is that the galvanic contact through the sweat ducts is given under both, the CC1 and CC2 electrodes, and that the state changes of the corresponding sweat duct memristors are relatively fast.

When v_{CC1} is positive, the memductance of the sweat duct memristor under CC1 decreases, while that under CC2 increases (since v_{CC2} has opposite polarity). Consequently, the current through the skin under CC2 will become dominant.

In the other half of the period, the opposite occurs, and the measured current will eventually mainly consist of the current through the skin under CC1. The rectified current was obtained from five subjects at 0.005 Hz. With subject L (only) it was possible to obtain a (almost) full wave rectified current even with a signal frequency of 0.5 Hz (Fig. 2a, bottom).

Currents that are (more or less) half wave rectified

The measured currents of some other subjects are more or less half wave rectified (Fig. 2b). If the galvanic contacts through the sweat ducts under both, the CC1 and CC2 electrodes, are achieved but one of both sweat duct memristors has a much lower initial memductance, a corresponding current like the one recorded from subject D (Fig. 2b, top) may be observed. In this example, the skin

memristor under CC1 initially presented a much lower memductance than that under CC2. The memductance under CC2 decreases in the second half of the period, while that under CC1 increases, but both end up at similar states. The resulting current is almost zero, since it is the sum of a negative current and a positive current of almost the same magnitude.

Subject B (see Fig. 2b middle plot) represents a case of half wave rectification under different conditions than subject D. The CC1 electrode was attached to the earlobe of Subject B (Variant A, see Fig. 1c) and it is known from the data in [22] that the skin under CC2 of subject B reflects the sweat duct memristor (pinched hysteresis loop with one pinched point, see Fig. 2c in [22]) while the skin under CC1 reflects the stratum corneum memristor (hysteresis loop with two pinched points, see Fig. S1 here). However, the memductances of both are within the same magnitude (maximum current of about 5 μ A at 1.2 V amplitude for both). In this example, the applied voltages will cause a memductance decrease under CC2 (sweat duct memristor) and a memductance increase under CC1 (stratum corneum memristor) within the first half of the period and the negative current through the skin under CC1 will dominate the measurement after a while. In the second half of the period, the memductances of both skin sites (under CC1 and CC2) will increase (since the stratum corneum memristor exhibits a memductance increase independent of the polarity of the applied voltage) and the currents through both skin sites will more or less cancel each other out. Similar results were achieved for the same subject also at 0.05 Hz (Fig. 2b bottom). A more detailed description that account for the oscillations in this specific example is given in the supplementary information.

Non-linear electrical currents that are not rectified

Subjects E and F in Fig. 2c represent the recordings in which neither frequency doubling, full wave rectification nor half rectification were observed. The obtained currents are non-linear (since the shape of the current is different from the applied sinusoidal voltage waveform). However, in case of subject E, the memductance under CC1 is initially much lower than that under CC2 and does not change significantly. The resulting current is more or less the current through the skin under CC2 which is dominated by the sweat duct memristor. For subject F, the whole measurement is dominated by the skin under CC1.

Evaluation over all subjects

A quantitative presentation of the results based on the parameter, r_{rec} , (see equation (7)) is shown in Fig. 3. The value of this parameter (representing the amount of rectification) becomes smaller as the frequency increases (see, for example, median and mean values). However, the outlier (which has a value of 65.9%) at 0.5 Hz is obtained

from subject L (see also Fig. 2a) and demonstrates that rectification can be obtained even at 0.5 Hz. The r_{rec} values of the (more or less) full wave rectified or frequency doubled currents (classification by optical inspection) were between 51.9% and 65.9%. The ratios of rectification at 0.005 Hz of subjects A and V, for example, are 59.13% and 54.11%, respectively (compare with Fig. 2). One exception was the current at 0.005 Hz of subject L which looked as it was more or less full wave rectified but had a value of 36.8%. The r_{rec} values of the currents that were considered to be half wave rectified were between 19.5% and 43%. The r_{rec} values of the currents of subjects D and B at 0.005 Hz and subject B at 0.05 Hz (see Fig. 2b) were 29.7%, 21.74%, and 34.14%, respectively. Subjects E and F (at 0.005 Hz, see Fig. 2c) obtained values of 11.83% and 14.33%, respectively.

Discussion

It is possible to rectify (more or less) electrical current with human skin. The adverbs “more or less” take into account that the obtained currents are not perfectly rectified as it would have been with a diode bridge. The sinusoidal

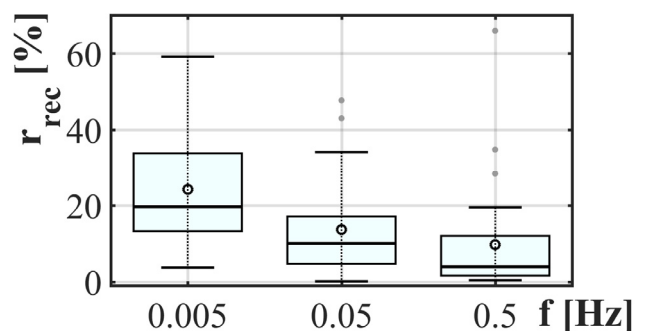


Fig. 3 | Boxplots reflecting the percentage of rectification of the current, i , normed with the average rectified value of a sinusoidal signal (r_{rec} , equation (7)). The boxplots are based on the evaluation of all subjects ($N=28$). These results are obtained from the recordings with different voltage frequencies (0.005 Hz, 0.05 Hz, and 0.5 Hz) and always shown for the first period (out of two). The horizontal line in the middle of each boxplot denotes the median; the circle indicates the mean value; and the whiskers indicate the 5% and 95% percentiles. The upper percentile is below 20% at 0.5 Hz which is in accordance with the observation that most subjects exhibited non-rectified currents at this frequency.

waveform is distorted since the recordings here are non-linear (see also [22]). The rectification (if it occurs) is based on the state changes of two memristors; if the skin under one electrode dominates the measurement (high memductance) during one half of the period and if the skin of the other electrode will become dominant after a while in the other half of the period, the current will be more or less full wave rectified. The state change of the sweat duct memristor is based on ion movements and takes time (as it does for memristors in general). There is always a delay until the other memristor will become dominant (and the polarity of the current switches) after the polarities of the voltages have switched. The lower the frequency of the voltages the

more time remains for the state changes to happen and the more rectified the current becomes. With higher frequencies less subjects exhibited rectified currents and the amount of rectification decreases (see Fig. 3). In general, as the frequency increases, the current becomes more linear. The electrical response of the skin at the forehead, for example, is likely to be completely linear when a sinusoidal voltage with 1 V amplitude and frequencies above 2 Hz is applied (see range of linear vs. non-linear measurements in Fig. 3 of [22]).

The classification whether the current was full wave rectified, half wave rectified or none of both was done by optical inspection of the current over time. The functioning of the overall circuit can also be distinguished by the corresponding voltage-current plots (see Fig. S2 in the supplementary information). A more qualitative measure was introduced by, r_{rec} , the ratio of rectification. This measure is with respect to a full wave rectified sinusoidal signal and can be used as a rough reference.

Based on the results here, it may be useful to classify currents that have r_{rec} values larger than 50% as (more or less) full wave rectified. If the r_{rec} value is between 20% and 50% the current may be classified as half wave rectified and below 20% as non-rectified. However, these are just orientation values. The currents obtained from two subjects that were not considered as rectified (by optical inspection) resulted in r_{rec} larger than 20% (21.6% and 22.4%, respectively). The currents were quite asymmetric with large area under the x-axis during one half of the period and with smaller but still noticeably large area above the x-axis during the other half of the period. It depends on the application whether the currents in these two examples should be classified as half wave rectified or not.

The existence of the sweat duct memristor (and the stratum corneum memristor) [22] has been demonstrated at the forehead and the earlobe. However, the galvanic contact through the sweat ducts was achieved from more subjects at the forehead than the earlobe (25 out of 28 subjects vs. 9 out of 28 subjects, see [22]). Since only 5 out of 12 subjects obtained either frequency doubling or half wave rectification when the electrode at the earlobe was used as CC1, another setup was used for the remaining 16 subjects in which CC1 was placed at the forehead close to CC2 (placed at the same time, see Fig. 1). However, also only 6 out of 16 subjects exhibited a rectified current in this setup. Since galvanic contact through the sweat ducts was usually obtained at the forehead under CC2 (see [22]) one could have expected similar conditions for the skin under CC1 in this setup (variant B) and consequently more subjects that exhibit rectified currents. However, each non-linear electrical measurement on human skin will also affect follow up measurements. Non-linear measurements were conducted at the skin under CC2 (experiment 1 presented in [22] and experiment 2 in which DC pulses were applied, unpublished

results) before this experiment started but not at the skin at the forehead under CC1. The memductance of the sweat duct memristor under CC2 increased with the before conducted experiments since sweat was pulled towards the skin surface which provided better current pathways. As a consequence, the initial memductance of the skin under CC2 was higher than that under CC1 for many subjects and if changes happened slowly, CC2 was dominating the measurements in both halves of the periods of the voltage (non-linear but non-rectified current). It was tried to reset the different initial conditions and to ensure galvanic contact through the sweat ducts by adding the one minute of workout at the stationary bike before the experiment started. It was shown that the non-linear electrical properties of human skin can change significantly before and after workout (see [24]). However, one minute on the stationary bike was very likely too short to cause any thermal sweating. If one repeats the experiment here with both electrodes at the forehead but without non-linear electrical measurements on only one of both electrodes before, one may obtain rectified currents from more subjects. Chances to obtain rectified currents are even higher if a workout that actually causes thermal sweating is included in the protocol.

Conclusion

The implemented memristor bridge can be seen as one application of the non-linear electrical properties of human skin and as part of non-linear electrical measurements in general. The functioning of the circuit (frequency doubling, full wave rectification, half wave rectification or none of these) depends on the conditions of the corresponding human skin memristors. The measurements will reveal how the physiological conditions of one skin site are in comparison to another skin site. Furthermore, since the half wave or full wave rectification only works under certain conditions, the memristor bridge circuit may be used in authentication systems. For example, one skin memristor may be replaced by an external reference memristor and access is only granted if the overall current is rectified. Other functions of the memristor bridge in general (like the generation of pulses that had similar shapes as neuronal pulses in [17] or synaptic weight programming in [15]) may be implemented with human skin, as well. However, as demonstrated here, it is in principle possible to realize a memristor circuit with human skin and further applications may be found later.

Competing interests

The author declares no competing interests.

Data and materials availability

The recorded data have been deposited with figshare. These data can be obtained free of charge from <https://figshare.com/s/46bcbe23a1e267a90521>.

References

1. Chua LO. Memristor-the missing circuit element. *IEEE Transactions on circuit theory*. 1971;18(5):507-19. <https://doi.org/10.1109/TCT.1971.1083337>
2. Chua LO. Everything you wish to know about memristors but are afraid to ask. *Radioengineering*. 2015;24(2):319. <https://doi.org/10.13164/re.2015.0319>
3. Chua LO. If it's pinched it's a memristor. *Semiconductor Science and Technology*. 2014;29(10):104001. <https://doi.org/10.1088/0268-1242/29/10/104001>
4. Strukov DB, Snider GS, Stewart DR, Williams RS. The missing memristor found. *nature*. 2008;453(7191):80. <https://doi.org/10.1038/nature06932>
5. Torrezan AC, Strachan JP, Medeiros-Ribeiro G, Williams RS. Sub-nanosecond switching of a tantalum oxide memristor. *Nanotechnology*. 2011;22(48):485203. <https://doi.org/10.1088/0957-4484/22/48/485203>
6. Yang JJ, Zhang M-X, Strachan JP, Miao F, Pickett MD, Kelley RD, et al. High switching endurance in TaO x memristive devices. *Applied Physics Letters*. 2010;97(23):232102. <https://doi.org/10.1063/1.3524521>
7. Zhu X, Su W, Liu Y, Hu B, Pan L, Lu W, et al. Observation of Conductance Quantization in Oxide-Based Resistive Switching Memory. *Advanced Materials*. 2012;24(29):3941-6. <https://doi.org/10.1002/adma.201201506>
8. Volkov AG, Tucket C, Reedus J, Volkova MI, Markin VS, Chua LO. Memristors in plants. *Plant signaling & behavior*. 2014;9(3):e28152. <https://doi.org/10.4161/psb.28152>
9. Gale E, Adamatzky A, de Lacy Costello B. Slime mould memristors. *BioNanoScience*. 2015;5(1):1-8. <https://doi.org/10.1007/s12668-014-0156-3>
10. Jo SH, Chang T, Ebong I, Bhadviya BB, Mazumder P, Lu W. Nanoscale memristor device as synapse in neuromorphic systems. *Nano letters*. 2010;10(4):1297-301. <https://doi.org/10.1021/nl904092h>
11. Indiveri G, Linares-Barranco B, Legenstein R, Deligeorgis G, Prodromakis T. Integration of nanoscale memristor synapses in neuromorphic computing architectures. *Nanotechnology*. 2013;24(38):384010. <https://doi.org/10.1088/0957-4484/24/38/384010>
12. Prezioso M, Merrih-Bayat F, Hoskins BD, Adam GC, Likharev KK, Strukov DB. Training and operation of an integrated neuromorphic network based on metal-oxide memristors. *Nature*. 2015;521(7550):61-4. <https://doi.org/10.1038/nature14441>
13. Merrih-Bayat F, Shouraki SB. Memristor-based circuits for performing basic arithmetic operations. *Procedia Computer Science*. 2011;3:128-32. <https://doi.org/10.1016/j.procs.2010.12.022>
14. Bickerstaff KA, Swartzlander EE. Memristor-based arithmetic. 2010 Conference Record of the Forty Fourth Asilomar Conference on Signals, Systems and Computers (ASILOMAR); 2010: IEEE. <https://doi.org/10.1109/ACSSC.2010.5757715>
15. Kim H, Sah MP, Yang C, Roska T, Chua LO. Memristor bridge synapses. *Proceedings of the IEEE*. 2012;100(6):2061-70. <https://doi.org/10.1109/JPROC.2011.2166749>
16. Cohen GZ, Pershin YV, Di Ventra M. Second and higher harmonics generation with memristive systems. *Applied Physics Letters*. 2012;100(13):133109. <https://doi.org/10.1063/1.3698153>
17. Pabst O, Schmidt T. Frequency dependent rectifier memristor bridge used as a programmable synaptic membrane voltage generator. *Journal of Electrical Bioimpedance*. 2013;4(1):23-32. <https://doi.org/10.5617/jeb.539>
18. Grimnes S. Skin impedance and electro-osmosis in the human epidermis. *Med Biol Eng Comput*. 1983;21(6):739-49. <https://doi.org/10.1007/BF02464037>
19. Yamamoto T, Yamamoto Y. Non-linear electrical properties of skin in the low frequency range. *Medical and Biological Engineering and Computing*. 1981;19(3):302. <https://doi.org/10.1007/BF02442549>
20. Panescu D, Webster JG, Stratbucker RA. A nonlinear electrical-thermal model of the skin. *IEEE Transactions on Biomedical Engineering*. 1994;41(7):672-80. <https://doi.org/10.1109/10.301734>
21. Johnsen GK, Lutken CA, Martinsen OG, Grimnes S. Memristive model of electro-osmosis in skin. *Phys Rev E Stat Nonlin Soft Matter Phys*. 2011;83(3 Pt 1):031916. <https://doi.org/10.1103/PhysRevE.83.031916>
22. Pabst O, Martinsen ØG, Chua LO. The non-linear electrical properties of human skin make it a generic memristor. *Scientific reports*. 2018;8(1):15806. <https://doi.org/10.1038/s41598-018-34059-6>
23. Martinsen ØG, Grimnes S. Bioimpedance and bioelectricity basics: Academic press; 2015.
24. Pabst O, Tronstad C, Martinsen ØG, editors. Instrumentation, electrode choice and challenges in human skin memristor measurement. *Engineering in Medicine and Biology Society (EMBC), 2017 39th Annual International Conference of the IEEE; 2017: IEEE*. <https://doi.org/10.1109/EMBC.2017.8037205>

Supplementary information

Rectifying memristor bridge circuit realized with human skin

Author: Oliver Pabst

Email: oliverpa@mail.uio.no

Detailed explanation for the half-wave rectification with a stratum corneum memristor and a sweat duct memristor

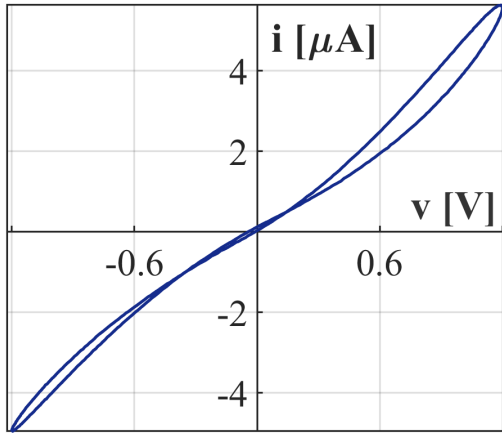


Fig. S1 | Alternating current (AC) voltage-current plot of subject B at the earlobe, shown for the third period of applied sinusoidal voltage with frequency of 0.05 Hz and amplitude of 1.2 V. These data (not shown before) are obtained from the experiment presented in [22]. The two pinched points are indication that the stratum corneum memristor (in parallel with the capacitive properties of the stratum corneum) is dominating the measurement and that the galvanic contact through the sweat ducts was not given (see [22]).

The oscillations of the current recorded from subject B in Fig. 2b are explained here. As demonstrated by Fig. S1, the skin of subject B under CC1 is dominated by the stratum corneum. Within the first half period of the applied voltages (from 0 s to 100 s in the middle plot of Fig. 2b, v_{CC1} is negative, v_{CC2} is positive) the memductance of the sweat duct memristor under CC2 was initially higher (since the current becomes more positive first) but decreases as the applied voltage increases. At the same time the memductance of the stratum memristor under CC1

increases. As soon as the memductance of the stratum corneum memristor under CC1 becomes larger than that of the sweat duct memristor under CC2, the overall current becomes negative. From 50 s to 100 s, as the voltages become smaller, the memductance of the stratum corneum memristor decreases instantly. As a consequence, the memductance of the sweat duct memristor under CC2 is slightly higher at the beginning of the second half of the period (at 100 s) and the overall current becomes more negative again. It seems the memductance of the stratum corneum memristor in this example increases faster than that of the sweat duct memristor, resulting in an overall current that is positive at around 150 s. As the voltages become smaller, the memductance of the stratum corneum under CC1 decreases again, and the memductance of the sweat duct memristor under CC2 is higher (resulting in a negative current again) close to the end of the period.

Average rectified value of a sinusoidal signal normed by its amplitude

The average of a rectified sinusoidal signal (normed to its amplitude) can be calculated by

$$\begin{aligned} r_{is} &= \frac{1}{AT} \int_0^T |A \sin(\omega t)| dt \\ &= \frac{2}{T} \int_0^{T/2} \sin(\omega t) dt \cdot \end{aligned} \quad (8)$$

Solving of the integral leads to

$$r_{is} = \frac{2}{T} \cdot \frac{2}{\omega} = \frac{2}{\pi} \approx 0.6366. \quad (9)$$

Voltage-current plots of the two-memristor bridge circuit realized with human skin

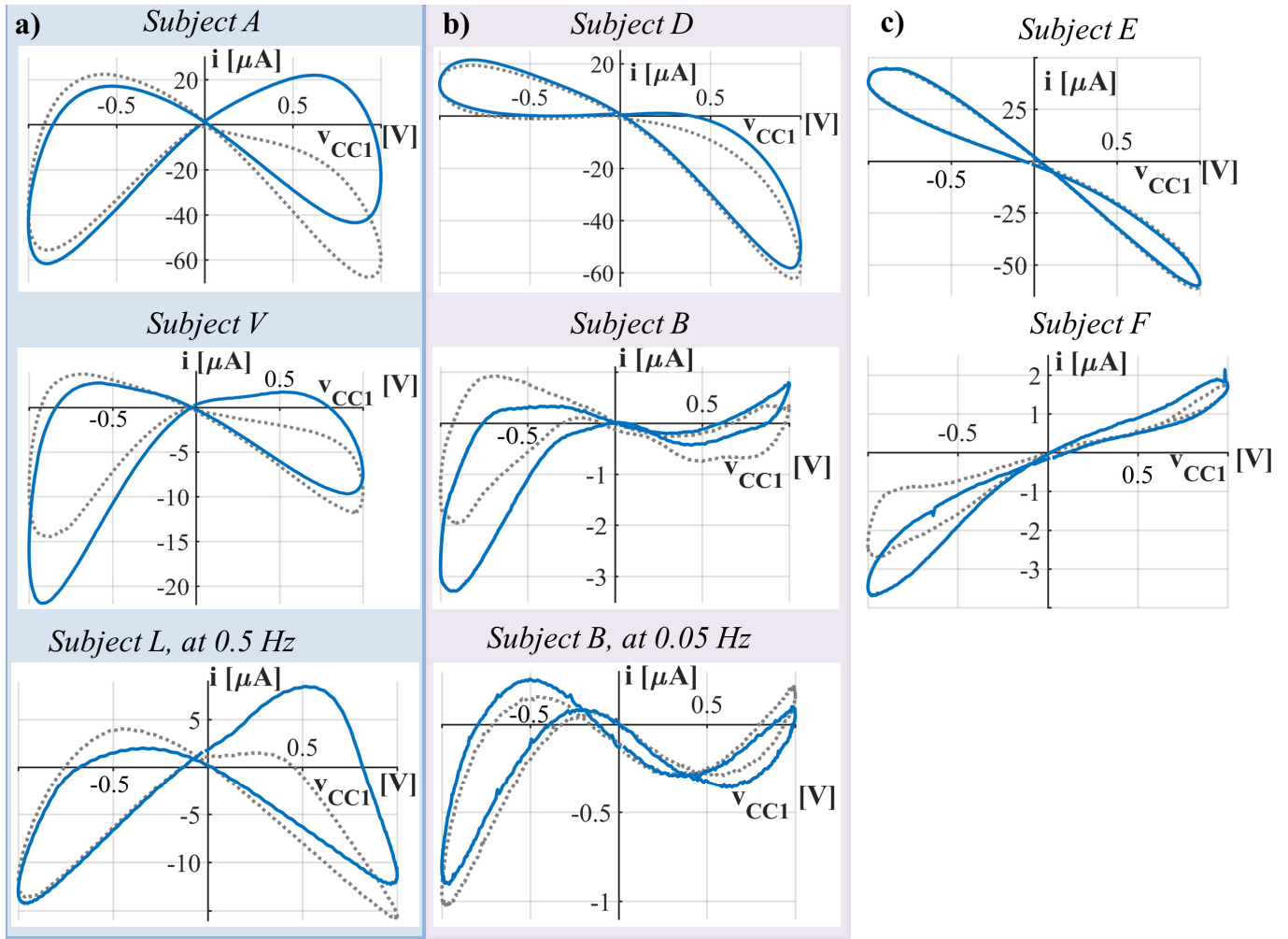


Fig. S2| Results from several subjects (voltage current plots). These are the results of the two-memristor bridge circuit shown for the same subjects that are presented in Fig. 2. Here the measured current, i , is plotted over the applied sinusoidal voltage v_{CC1} (on CC1); the sign of the applied sinusoidal voltage v_{CC2} under CC2 was opposite. Even though pinched hysteresis loops may cross the second and fourth quadrant in this presentation (plotted with regard to v_{CC1} , but not v_{CC2}) it does not mean that the corresponding memristor circuit is active. The plot of subject E, for example, just means that the skin under CC2 is dominating the measurement. The results are shown over two periods (the grey dotted plot presents the first period and the blue solid plot presents the second period). In the top and middle line, the results of the recordings with a voltage frequency of 0.005 Hz are shown. (a) Subject A, V at 0.005 Hz and Subject L at 0.5 Hz; all exhibited (more or less) full-wave rectified currents in Fig. 2. The corresponding V-I plots show pinched hysteresis loops with large lobe areas in the third and fourth quadrant but relative small areas in the first and second. (b) Subject D and B at 0.005 Hz and subject B at 0.05 Hz; all exhibited more or less half wave rectified currents in Fig. 2. The corresponding V-I plots show pinched hysteresis loops with relative large lobe area in either the third or fourth quadrant. Within the other quadrant (either fourth or third quadrant, respectively), the corresponding branch of the loop does not span a large area but is close to the x-axis instead. (c) Subject E and F. Since one skin site (under CC1 or CC2) dominates each measurement, the V-I plots reflect the pinched hysteresis loops of single skin memristors.